

Adaptive Impulse Noise Suppression in OFDM Systems

J. Radić, N. Rožić

Department of Electronics, University of Split,

Ruđera Boškovića bb, 21000 Split, Croatia, phone: +385 21 305635, e-mail: radic@fesb.hr

Introduction

Digital data transmitting, based on orthogonal carrier modulation is relatively old. Actually, it is a special case of parallel transmission realized by frequency division multiplex (FDM). In classical FDM, channel separation is based on non-overlapping frequency bands. Each subchannel is modulated with different carrier frequency. Resulting spectrum is superposition of subchannels spectrum that are non-overlapped. The main disadvantage of this scheme is in a poor spectrum efficiency. An improvement of the described FDM scheme can be achieved by choosing the orthogonal set of carriers. In that case, spectrum overlapping is permitted with the minimal interference between the adjacent channels, while the channel separation is maintained. Recently, an orthogonal frequency division multiplexing technologies (OFDM) is becoming very popular in wireless communication systems. Today it is implemented in DVB-T and WiMAX standards. Implementation is relatively simple by applying IDFT and DFT in transmitter and receiver respectively [1].

Performance analysis of the communication system based on parallel transmission has been reported in [2]. The motivation for implementing a system for parallel transmission is in efficient utilization of the transmission media that results in easier equalization, and in increased immunity on impulse noise [3]. Impulse noise immunity comes from extended symbol duration, since the impulse noise is usually of very short duration compared to symbol duration in parallel transmission.

Impulse noise immunity of the orthogonally multiplexed QAM system has been reported in [4]. However, in [5] comparison of the multicarrier modulation system (MMC) and single carrier (SC) is performed and the simulation results show better performance of the SC system than the MCM for higher impulse rates and power.

Different approaches for impulse noise suppression are proposed in literature. An iterative approach, where M largest samples of the estimated noise are subtracted from the received signal, is proposed in [6]. This method is based on the assumption that the largest amplitudes in the noise estimation are probably impulse noise samples. In addition, an iterative method for decoding complex number codes in impulse noise environment is described in

[7]. Two estimators, in time and frequency, domain exchange information on impulse noise between themselves. Both estimators uses only partial information for estimation like in turbo coding. An algorithm for impulse noise compensation in frequency domain is proposed in [8]. In this method author propose impulse noise detection based on threshold that is calculated taking into account estimation of the noise variance.

Calculation of the optimum threshold for impulse noise detection is reported in [9]. Most of the proposed methods require some knowledge on impulse noise parameters, with the exception of method proposed in [6].

In this paper we propose an iterative method for impulse noise suppression based on a priori information in frequency domain and variable threshold for impulse noise samples detection in time domain. We found that the threshold can be defined based on signal to noise ratio when signal is not affected with impulse noise. For that reason, the proposed method does not require estimation of the impulse noise parameters for moderate impulse noise power level.

The rest of the paper is organized as follows. First in Section II. we analyze system and channel model, as well as the impulse noise model. This is followed with the proposed system description in Section III. In Section IV., we discuss simulation and results and in Section V. give some concluding remarks.

System and Channel Modeling

We use baseband signaling model for system description. Received baseband samples in frequency domain of the OFDM frame after removing the cyclic prefix and performing FFT are:

$$Y[n] = H[n]X[n] + W[n] + I[n], \quad n = 0, 1, \dots, N-1 \quad (1)$$

where $Y[n]$, $H[n]$, $X[n]$, $W[n]$ and $I[n]$ denotes samples of the received signals $\mathbf{Y} = [Y[0], Y[1], \dots, Y[N-1]]$, channel coefficients $\mathbf{H} = [H[0], H[1], \dots, H[N-1]]$, transmitted symbols $\mathbf{X} = [X[0], X[1], \dots, X[N-1]]$, additive white Gaussian noise (AWGN) $\mathbf{W} = [W[0], W[1], \dots, W[N-1]]$ and impulse noise samples $\mathbf{I} = [I[0], I[1], \dots, I[N-1]]$. Capital letter N is length of the OFDM frame. For channel

modeling we use multipath frequency selective channel model [10]

$$\mathbf{H}[n] = \sum_{s=1}^S \alpha[s] \exp \left[-j \frac{2\pi}{N} \left(n - \frac{N_d}{2} \right) \frac{\tau[s]}{T} \right], \quad (2)$$

where S is number of paths, N_d is number of data and pilot carriers, T is time band between samples, and $\tau[s]$ is time delay of the s -th path. Here we assume that N_d central carriers are reserved for data and pilots, whereas the remaining are used as zero carriers i.e. guard band in frequency domain. Coefficients $\alpha[s]$ are zero mean independent Gaussian samples, and it is assumed that $\sum_{s=1}^S E[|\alpha[s]|^2] = 1$, where $E[\cdot]$ is the expectation operator. The N_d central coefficients $X[n]$ are complex valued constellation points, representing data or pilot symbols to be transmitted. Values of the data carriers depend on modulation type (MPSK, MQAM e.t.c.), and are elements of the set $\mathbf{X} = \{X_0, X_1, \dots, X_{[M-1]}\}$, where M is number of symbols in constellation diagram. It is assumed for data carriers that $E_s = E[X[n] X^*[n]]$, where E_s

denotes energy per symbol, while the energy per bit is $E_b = E_s / \log_2 M$. Noise samples $W[n]$ are independent zero mean Gaussian distributed samples, of variance $\sigma_n^2 = N_0 / 2$ per complex dimension, where $N_0 / 2$ denotes double side spectral noise density. Usual approach for impulse noise modeling in time domain is based on Middleton or Bernoulli-Gaussian model [11] and [5]. In this paper we use Bernoulli-Gaussian impulse noise model. Vector of impulse noise samples in frequency domain is DFT of the impulse noise samples in time domain, i.e. $\mathbf{i} = [i[0], i[1], \dots, i[N-1]]$, $\mathbf{I} = \text{DFT}\{\mathbf{i}\}$. Bernoulli-Gaussian noise process is defined as:

$$i[n] = b[n]g[n], \quad (3)$$

where $b[n]$ denotes independent identically distributed samples from Bernoulli distribution i.e. $b[n] \in \mathbf{B} = \{0, 1\}$, and $\Pr\{b[n] = 1\} = p$. $g[n]$ denotes complex zero mean independent identically distributed samples from Gaussian distribution variance of σ_g^2 . Bernoulli Gaussian noise is applicable for modeling noise generated with hairdryer [8].

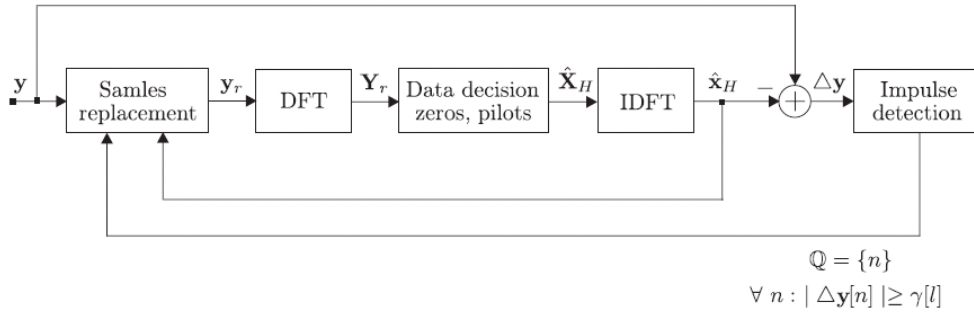


Fig. 1. Block scheme of system for impulse noise suppression

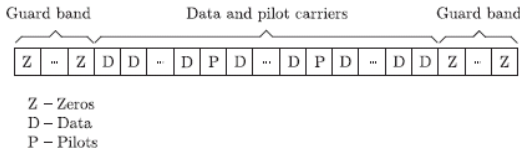


Fig. 2. OFDM frame structure

The proposed System for Impulse Noise Suppression

The basic idea of the proposed method for impulse noise suppression is in combining the signal properties in frequency and time domain (Fig. 1). OFDM frame usually contain three carrier types (Fig. 2). Central placed carriers are reserved for data and pilots while the remaining serves as guard band in frequency domain, and their values are set to zeros. Pilot carriers values are predefined values and the receiver estimate the channel coefficients based on them. Data carriers values depend on applied modulation. After removing a cyclic prefix, received signal in time domain is obtained $\mathbf{y} = \text{IDFT}\{\mathbf{Y}\}$.

Samples of the received signal \mathbf{y} , which are detected as corrupted with impulse noise, are replaced with the samples of the reestimated signal $\hat{\mathbf{x}}_H$. By replacing the samples of the signal \mathbf{y} with the samples of the signal $\hat{\mathbf{x}}_H$, reconstructed signal in time domain is obtained $\hat{\mathbf{y}}_r$. Procedure can be iteratively repeated.

In first iteration, signal $\hat{\mathbf{y}}_r$ is equal to \mathbf{y} , since positions of the impulse noise are unknown. Now, vector $\hat{\mathbf{y}}_r$ is transformed in frequency domain, and signal $\hat{\mathbf{Y}}_r = \text{DFT}\{\hat{\mathbf{y}}_r\}$ is obtained. After that, a priori information is used for generating signal $\hat{\mathbf{X}}_H$. Zero carriers are set to zero

$$\hat{X}_H[n] = 0, \quad \forall n \in \mathbf{Z}_c, \quad (4)$$

where \mathbf{Z}_c denotes set of zero carriers indices. Pilot carriers are set to values

$$\hat{X}_H[n] = H[n]P, \quad \forall n \in \mathbf{P}_c, \quad (5)$$

where \mathbf{P}_c denotes set of pilot carriers indices, and P denotes pilot carriers values. Pilot carrier values are multiplied with the corresponding channel coefficients $H[n]$, since the signal $\hat{\mathbf{X}}_H$ is not equalized. MAP measure is used for transmitted data decision:

$$\hat{X}_H[n] = \arg \min_{\mathbf{X}} \{Y_r[n] - XH[n]\} H[n], \quad \forall X \in \mathbf{X}, \quad \forall, \quad (6)$$

where \mathbf{D}_c denotes set of data carriers indices. Frequency domain signal $\hat{\mathbf{X}}_H$ is transformed by means of IDFT in time domain unequalized signal $\hat{\mathbf{x}}_H$. The iterative procedure is realized by replacing samples of the received signal \mathbf{y} , that are stor in buffer in first iteration, and

detected as impulse noise, with the samples of the signal $\hat{\mathbf{x}}_H$:

$$\begin{cases} y_r^{(l)}[n] = \hat{x}_H^{(l)}[n], & \forall n \in \mathbf{Q}, \\ y_r^{(l)}[n] = y_r^{(l-1)}[n], & \forall n \in \{0, 1, \dots, N-1\} \setminus \mathbf{Q}, \end{cases} \quad (7)$$

where \mathbf{Q} denotes set of the impulse noise positions. Estimation of impulse noise positions will be explained in the next subsection. The new iteration proceed as described with the signal $\mathbf{y}_r^{(l)}$.

Impulse noise positions estimation

Positions of the noise impulses can be estimated from the absolute value of the difference between the received signal and reconstructed signal.

$$\begin{aligned} |\Delta \mathbf{y}^{(l)}| &= |\mathbf{y} - \hat{\mathbf{x}}_H^{(l)}|; \\ &= |\mathbf{y} - \mathbf{x}_H + \mathbf{e}^{(l)}|. \end{aligned} \quad (8)$$

By assuming algorithm convergence, reconstructed signal converge to the original signal, thus the difference between the received signal and reconstructed converge to noise. Since the noise is superposition of the Gaussian noise and impulse noise, positions of the impulse noise can be estimated based on predetermined threshold. Here, we assume that the deviation of the impulse noise is much greater than the deviation of the Gaussian noise. Under the assumption that the random variable \mathbf{e} is Gaussian distributed, reliability i.e. deviation σ_e that follows directly from that variable defines the threshold for impulse noise position detection. Deviation σ_e of the random variable $e[n]$ can be calculated from the probability of error (18).

$$\sigma_e = \sqrt{\frac{1}{N} \sigma_E} = \sqrt{\frac{2p_e}{N}}, \quad (9)$$

where σ_E denotes deviation of the random variable $E[n]$.

In appendix, it is shown that the deviation σ_e approximately exponentially decreases during iterations. Since the impulse noise parameters are unknown, at first iteration, threshold is proportional with the Gaussian noise deviation.

$$\gamma[l] = A \sqrt{N_o/2} 0.8^l, \quad (10)$$

where A denotes fixed value which is experimentally determined by minimizing the symbol error rates.

$$\mathbf{Q} = \{n\}, \forall n : |\Delta \mathbf{y}^{(l)}[n]| \geq \gamma[l], \quad (11)$$

where \mathbf{Q} denotes set of estimated impulse noise positions based on threshold, $\boldsymbol{\gamma} = [\gamma[0], \gamma[1], \dots, \gamma[D-1]]$ is vector of thresholds, D is number of iterations and l denotes current iteration.

Simulation results

In all simulations we assume 256 carriers in OFDM frame, 64 guard band zeros and 0 pilot carriers. We assume perfectly knowledge of channel parameters in the receiver and we take that the duration of the cyclic prefix is equal

or larger than channel impulse response. Channel parameters are independent among the different OFDM frames. Channel parameters in our simulation are presented in Table 1. Modulation of the subcarrier is 16-QAM. Iterative procedure is performed with 5 iterations.

We present simulation results for three different simulations scenarios. In first, symbol error rate (SER) versus thresholds parameters A and k are presented, for method with threshold adaptation and method with constant threshold, respectively. In the second, SER versus E_b/N_0 is presented and in the third scenario, SER versus E_b/N_0 for 1 to 5 iterations is presented. Performance of the algorithm with the variable threshold are compared with the same algorithm but with constant threshold which is given by $\gamma_c = k\sqrt{N_o/2}$.

Fig. 3 and Fig. 4 show SER versus thresholds parameters A and k for $p = 0.1$, $\sigma_g^2/\sigma_n^2 = 100$ and 10 respectively. Fig. 3 shows that variations of threshold parameter A from 0.5 to 0.7 does not affect significantly SER, particularly at signal noise ratio higher than 25 dB. Opposite to this situation, parameter k which gives minimal SER spans from 0.45 to 0.35, depending on signal to noise ratio. Fig. 4 shows the situation with relatively small impulse noise power. The same values of parameter A variation as in situation with large impulse noise, minimizes the SER. However optimal k varies from 0.25 to 0.2, and it differs significantly in comparison with optimal values for large impulse noise. From the presented simulations it is obvious that the proposed algorithm is superior comparing to the algorithm with the constant threshold. Due to low sensitivity of the SER on the threshold parameter A for low and moderate σ_g^2/σ_n^2 ratio, estimation of the impulse noise parameters p and σ_g^2 is not necessary.

Fig. 5 and Fig. 6 show the SER vs. E_b/N_0 for method with variable and constant thresholds. Performance of the system without impulse noise, as for scenarios without using algorithm for impulse noise suppression are also displayed. Simulations are performed for $p = 0.1$, $\sigma_g^2/\sigma_n^2 = 100$, and 10 respectively. As can be seen from the figures, both methods produce significantly better results in comparison with the conventional decoder. For moderate σ_g^2/σ_n^2 ratio, performance gain is larger with method with adaptive threshold parameter. However, at low σ_g^2/σ_n^2 ratio both methods provide same capabilities for impulse noise suppression.

It is interesting to note that at lower σ_g^2/σ_n^2 ratio, method with adaptive threshold performs better impulse noise suppression than at lower σ_g^2/σ_n^2 ratio. The main reason for this is in detection impulse noise positions. At lower σ_g^2/σ_n^2 ratios impulse noise is masked with Gaussian noise and it is hard to detect difference between impulse noise and Gaussian noise.

Fig. 7 and Fig. 8 show the SER vs. E_b/N_0 depending on iterations for method with constant and adaptive thresholds respectively. In both figures, probability of impulse noise is $p = 0.2$, and $\sigma_g^2/\sigma_n^2 = 100$.

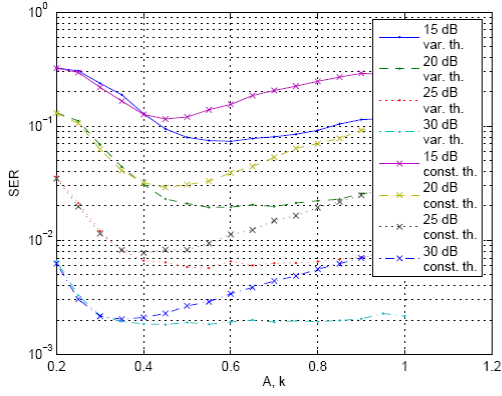


Fig. 3. SER vs. threshold parameters for method with adaptive and fixed threshold, $p = 0.1$ and $\pi = 0.1$, $\sigma_g^2 / \sigma_n^2 = 100$

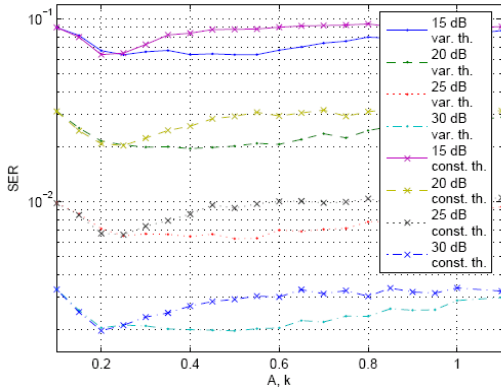


Fig. 4. SER vs. threshold parameters for method with adaptive and fixed threshold, $p = 0.1$ and $\pi = 0.1$, $\sigma_g^2 / \sigma_n^2 = 10$

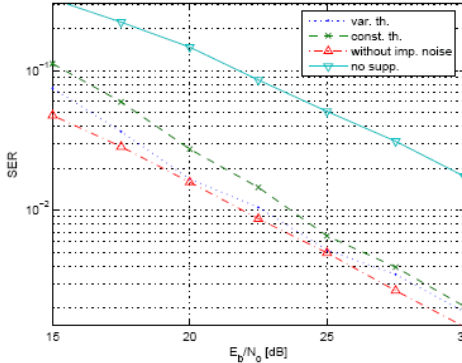


Fig. 5. SER vs. E_b/N_0 in channel with Bernoulli-Gaussian impulsive noise, $p = 0.1$ and $\pi = 0.1$, $\sigma_g^2 / \sigma_n^2 = 100$

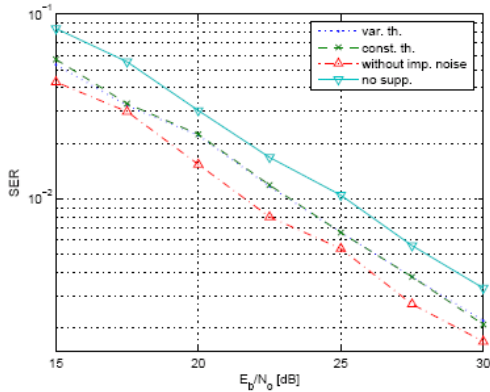


Fig. 6. SER vs. E_b/N_0 in channel with Bernoulli-Gaussian impulsive noise, $p = 0.1$ and $\pi = 0.1$, $\sigma_g^2 / \sigma_n^2 = 10$

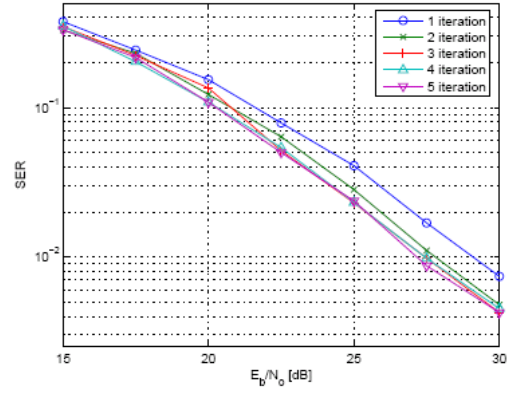


Fig. 7. SER vs. E_b/N_0 for method with fixed threshold and number of iteration as parameter, $\pi = 0.2$, $\sigma_g^2 / \sigma_n^2 = 100$

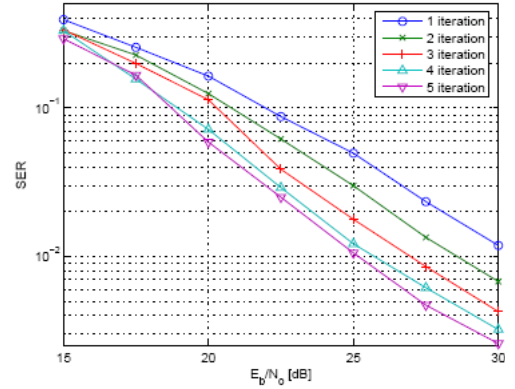


Fig. 8. SER vs. E_b/N_0 for method with variable threshold and number of iteration as parameter, $\pi = 0.2$, $\sigma_g^2 / \sigma_n^2 = 100$

The method with variable threshold is inferior during the first two iterations, but for 3rd and higher iterations it is superior comparing to method with constant threshold. Also, in method with variable threshold it is reasonable to apply 5 iterations, while in the method with constant threshold it is not, since after 3rd iteration performance is only slightly better.

Table 1. Channel parameters

Path, s	Power [dB]	Delay τ [μ s]
1	-4	0
2	-3	0.1
3	0	0.3
4	-2.6	0.5
5	-3	0.8
6	-5	1.1
7	-7	1.3
8	-5	1.7
9	-6.5	2.3
10	-8.6	3.1
11	-11	3.2
12	-10	5

Conclusions

In this paper, we propose a novel approach for impulse noise suppression in OFDM communication systems. The method is based on iterative algorithm, by combining the a priori knowledge on signal properties in the frequency domain and estimation of the noise impulses with adaptive

threshold in time domain. In frequency domain, OFDM signal usually contains zeros in guard band and pilot tones and positions of the noise samples are determined by comparing the received signal with estimated signal in time domain. Samples that are detected as impulse noise are replaced with the samples of the estimated signal in the time domain. The proposed method does not require estimation of the impulse noise parameters for wide variations in impulse noise characteristics. Simulation results show that the proposed system efficiently compensate the impact of the impulse noise even in the case of strong impact of noise impulses. Furthermore, estimation of the impulse noise properties should not be performed for low and moderate relative impulse noise power since the SER is not sensitive on threshold.

Appendix

For a sake of simplicity, we assume flat fading channel, and OFDM frame without zeros and pilots. Received signal in time domain is given by:

$$y_r^{(l)}[n] = \begin{cases} x[n] + w[n], & \forall n \in \mathbf{O} \setminus \mathbf{Q}, \\ \hat{x}^{(l-1)}[n], & \forall n \in \mathbf{Q}, \end{cases} \quad (12)$$

where, $\hat{x}[n]$ denotes hard decision of the transmitted symbols in time domain, $e[n]$ is the error i.e. $\hat{x}[n] = x[n] - e[n]$, l is the current iteration index. \mathbf{O} denotes OFDM frame index, \mathbf{Q} is set of impulse noise positions, $w[n]$ and $i[n]$ are Gaussian and impulse noise samples respectively. Equation (12) can be written in matrix notation as:

$$\begin{aligned} \mathbf{Y}_r^{(l)} &= \mathbf{A}_Q \mathbf{x} + \mathbf{A}_Q \mathbf{w} + \mathbf{A}_Q \hat{\mathbf{x}}^{(l-1)} = \\ &= \mathbf{x} + \mathbf{A}_Q \mathbf{w} - \mathbf{A}_Q \mathbf{e}^{(l-1)}, \end{aligned} \quad (13)$$

where $\mathbf{A}_Q = \text{diag}\{\mathbf{q}\}$, $q[k] = 1$ for all $k \in \mathbf{Q}$, $q[k]=0$ for all $k \in \mathbf{O} \setminus \mathbf{Q}$ and $\mathbf{A}_Q^- = \mathbf{I}_N - \mathbf{A}_Q$. \mathbf{I}_N denotes unit matrix of size N . Taking the Fourier transform of (13), we obtain

$$\mathbf{Y}_r^{(l)} = \mathbf{X} + \mathbf{F} \mathbf{A}_Q \mathbf{F}^- \mathbf{W} - \mathbf{F} \mathbf{A}_Q \mathbf{F}^- \mathbf{E}^{(l-1)}, \quad (14)$$

where $\mathbf{F} = \text{DFT}\{\mathbf{I}_N\}$, and $\mathbf{F}^- = \text{DFT}\{\mathbf{I}_N\}$ are matrices that define Fourier and inverse Fourier transform respectively. Second and third part of the Eq. (14) represent noise i.e. $\mathbf{Z}^{(l)} = \mathbf{A}^- \mathbf{W} - \mathbf{A}^+ \mathbf{E}^{(l)}$, where $\mathbf{A}^- = \mathbf{F} \mathbf{A}_Q \mathbf{F}^-$ and $\mathbf{A}^+ = \mathbf{F} \mathbf{A}_Q \mathbf{F}^-$. Further, let

$$\begin{cases} Z_1[k] = \sum_{n=0}^{N-1} a^+[k, n] W[n], \\ Z_2^{(l)}[k] = - \sum_{n=0}^{N-1} a^-[k, n] E^{(l)}[n], \end{cases} \quad (15)$$

where $a^+[k, n]$ and $a^-[k, n]$ are elements of matrix \mathbf{A}^- and \mathbf{A}^+ . $Z_1[k]$ is zero mean Gaussian random variable with variance $\sigma_{Z_1}^2 = \sigma_w^2 \sum_{n=0}^{N-1} |a^+[k, n]|^2$ where σ_w^2 denotes variance of $W[n]$. It is not easy to found distribution of the $Z_2^{(l)}[k]$ since $E[n]$ are correlated with the respect of n . We found that the $Z_2^{(l)}[k]$ can be very well fitted with the generalized Gaussian distribution (GGD). Zero mean GGD

is defined with shape parameter λ and variance of the distribution σ_{GG}^2 . Probability density function of the GGD takes the form:

$$\begin{aligned} p_{Z_2}(x) &= \frac{\lambda}{2 \psi \Gamma(\frac{1}{\lambda})} e^{-\left(\frac{|x|}{\psi}\right)^\lambda}, \\ \psi &= \sqrt{\sigma_{GG}^2 \frac{\Gamma(\frac{1}{\lambda})}{\Gamma(\frac{3}{\lambda})}}, \end{aligned} \quad (15)$$

where Γ denotes gamma function:

$$\Gamma(\omega) = \int_0^\infty v^{\omega-1} e^{-v} dv, \quad \omega > 0. \quad (17)$$

Table 2. Parameters of the Generalized Gaussian noise and comparison of BER obtained by theory and simulation

Iter.	σ_{GG}	λ	BER, th.	BER, sim.	σ_e th.	σ_e sim.
$E_b/N_0 = 4$ dB, $\sigma_i^2/\sigma_w^2 = 50$, 8 impulses						
0.	-	-	-0.44	-0.44	0.1065	0.1065
1.	0.1756	1.8	-0.78	-0.68	0.0720	0.0808
2.	0.0789	1.4	-1.08	-0.87	0.0520	0.0649
3.	0.0436	1.1	-1.28	-1	0.0405	0.0559

Now, distribution p_Z can be approximately calculated by taking the numerical convolution of the random variables p_{Z_1} and p_{Z_2} , i.e. $p_Z = p_{Z_1} \otimes p_{Z_2}$. The probability of symbol error from the (16), for the 4 QAM, OFDM system:

$$p_e = 2 p_{tail}(1 - p_{tail}) + p_{tail}^2 \quad (18)$$

where

$$p_{tail} = \int_{x_r}^\infty p_Z(x) dx, \quad (19)$$

$x_r = 2 E_s x_r = 2 E_s / \sqrt{2}$ and E_s is energy per symbol.

In Table 2 are presented theoretic and simulation results for the OFDM system with 64 carriers and 4 QAM modulation, with 8 impulses of the impulse noise, $\sigma_i^2/\sigma_w^2 = 50$ and $E_b/N_0 = 4$ [dB].

References

1. **Weinstein S., Ebert P.** Data Transmission by Frequency-Division Multiplexing Using the Discrete Fourier Transform, IEEE Transactions on Communication Technologies // Com, 1971. – No. 5(19). – P. 628–634.
2. **Saltzberg B.** Performance of an Efficient Parallel Data Transmission System, IEEE Transactions on Communication Technologies // Com, 1967. – No. 6(15). – P. 805–811.
3. **Bingham J. A. C.** Multicarrier Modulation for Data Transmission: An Idea Whose Time Has Come. – IEEE Commun // Com, 1990. – P. 5–14.
4. **Hirosaki B., Hasegawa S., Sabato A.** Advanced Groupband Data Modem Using Orthogonally Multiplexed QAM

- Technique, IEEE Trans. On Commun // Com, 1987. – No. 6(34). – P. 587–592.
5. **Ghosh M.** Analysis of the Effect of Impulse Noise on Multicarrier and Single Carrier QAM Systems, IEEE Trans. on Commun // Com, – 1996. – No. 2(44). – P. 145–147.
 6. **Dhibi Y., Kaiser T.** Impulsive Noise in UWB Systems and its Suppression // Monet, 2006. – No. 4(11). – P. 441–449.
 7. **Haring J., Vinck A. J. H.**, Iterative Decoding of Codes Over Complex Numbers for Impulsive Noise Channels // IEEE Transactions on Information Theory, 2003. – No. 5(49). – P. 1251–1260.
 8. **Zhidkov S. V.**, Impulsive Noise Suppression in OFDM-based Communication Systems // IEEE Trans. on Consumer Electronics, 2003. – No. 4(49). – P. 944–948.
 9. **Armstrong J., Suraweera H. A.**, Impulse noise mitigation for OFDM using decision directed noise estimation // IEEE International Symposium on Spread Spectrum Techniques and Applications (ISSSTA), 2004. – P. 174–178.
 10. **Simeone O., Ness Y. B., Spagnolini U.** Pilot-Based Channel Estimation for OFDM Systems by Tracking the Delay-Subspace // IEEE Trans. Wireless Commun, 2004. – No. 1(3). – P. 315–325.
 11. **Spaulding A., Middleton D.** Optimum Reception in an Impulsive Interference Environment-Part I: Coherent Detection // IEEE Trans. on Commun, 1977. – No. 9(25). – P. 910–923.

Received 2009 02 17

J. Radić, N. Rožić. Adaptive Impulse Noise Suppression in OFDM Systems // Electronics and Electrical Engineering. – Kaunas: Technologija, 2010. – No. 1(97). – P. 3–8.

This paper presents a novel approach to adaptive impulse noise suppression in OFDM system. Our method is based on the analytically modeled threshold whose adaptation, in a contrast to known approaches, does not require computation of the impulse noise parameters in each iteration. The proposed method utilizes a priori knowledge in frequency domain in order to reconstruct samples corrupted by impulse noise. A priori information in frequency domain includes zeros in guard bands, pilot symbols as well as parameters of the data carriers constellation. The proposed algorithm reconstructs signal samples corrupted by impulse noise based on hard decisions in the frequency domain and detects the noise impulses through comparison of the reconstructed signal and the received signal. Decision regarding the impulse sample is based on the threshold whose value is decreasing exponentially from iteration to iteration. The exponent (decreasing rate) is determined based on the reliability of impulse calculated from pdf of random variable calculated from a difference between reconstructed signal and the received signal. The performances of the proposed system are evaluated through simulation which confirms theoretical analysis. Il. 7, bibl. 11, tabl. 2 (in English; abstracts in English, Russian and Lithuanian).

Ю. Радич, Н. Рожич. Применение ослабления импульсных шумовых сигналов в системах OFDM // Электроника и электротехника. – Каunas: Технология, 2010. – № 1(97). – С. 3–8.

Описывается адаптивное ослабление импульсных шумов в системах с применением OFDM. Данный метод основан на восстановлении сигнала после воздействия импульсных шумов с учетом известных исходных параметров сигнала. Амплитуда сигнала изменяется экспонентно в зависимости от числа итераций. Показатель экспоненты рассчитывается с учетом разности восстановленных и полученных сигналов. Проведен теоретический анализ моделирования сигналов. Ил. 7, библи. 11, табл. 2 (на английском языке; рефераты на английском, русском и литовском яз.).

J. Radić, N. Rožić. Impulsinių triukšmų adaptyviojo slopinimo taikymas OFDM sistemose // Elektronika ir elektrotechnika. – Kaunas: Technologija, 2010. – Nr. 1(97). – P. 3–8.

Išnagrinėtas impulsinių triukšmų adaptyvinis slopinimas OFDM sistemose. Tyrimo metodai pagrįsti triukšmo ribų modeliavimu, kai nebūtina perskaičiuoti impulsinių triukšmų parametrų kiekvienos iteracijos metu. Siūlomas metodas grindžiamas signalo atkūrimu taikant žinomus pradinius signalo parametrus po impulsinio triukšmo poveikio. Nustatyta, kad signalo amplitudė kinta pagal eksponentinį dėsnį priklausomai nuo iteracijų skaičiaus. Eksponentės mažėjimo laipsnis apskaičiuojamas įvertinus skirtumus tarp atkurtojo ir gautojo signalų. Atliktas signalų modeliavimas, pagrindžiantis teorinę analizę. Il. 7, bibl. 11, lent. 2 (anglų kalba; santraukos anglų, rusų ir lietuvių k.).